Binary Phase Behavior of Perfluoroalkanes

Douglas L. Dorset

Electron Diffraction Department, Medical Foundation of Buffalo, Inc., 73 High Street, Buffalo, New York 14203. *Received June 6, 1989; Revised Manuscript Received August 21, 1989*

ABSTRACT: The binary phase behavior of perfluoroalkanes has been investigated in terms of their self-interaction in polydisperse compositions and their respective interactions with alkanes and diblocks composed of alkane and perfluoroalkane segments. The formation of solid solutions in perfluoroalkanes proceeds according to the molecular volume constraints found for *n*-paraffins, and, like the paraffins, fractionation may proceed through an intermediate incommensurate solid structure as the chain length difference is gradually increased. There is no cosolubility of perfluoroalkanes with alkanes, in either the solid or the liquid phase. Accordingly, linear diblocks of the two separate species can be seen to behave as detergent-like molecules, i.e. with normal hydrophobic behavior of the alkyl chain, but replacing the usual hydrophilic moiety with a "fluorophilic" group.

Introduction

Because polydispersity is a common factor in natural and synthetic compounds containing linear chain segments, considerable effort has been made in order to understand the effect of homologous impurities on the physical properties of such materials in terms of crystal packing. An already extensive set of thermal and diffraction data from binary alkane solids was reviewed by Mnyukh[1] in 1960 and served as a basis for structural generalizations by Kitaigorodskii.[2] More recently the use of epitaxial orientation techniques has enabled us to examine the microcrystalline state of paraffins in terms of local crystal packings to find that some interpretations made from strictly bulk measurements needed to be revised.[3] For linear alkanes, a series of crystalline arrays is found to exist from the stable solid solution to the fully separated eutectic, as evidenced by the existence of intermediate incommensurate lattice structures grown from metastable solid solutions.[4] The presence and concentration of defect structures has also been described, based upon vibrational spectroscopic measurements.[5,6]

Although perfluoroalkanes are oligomers of the commercially important poly(tetrafluoroethylene), more data are needed to describe their binary phase behavior in comparison to paraffins, e.g. what chain length differences are tolerated in a solid solution and what structural intermediates are found when such binary compositions fractionate. (Preliminary studies have already been made, primarily to determine the solubility of the infinite polymer in perfluoroalkanes etc.[7]) Additionally, a fascinating group of diblock compounds composed of alkane and perfluoroalkane segments have been synthesized and studied recently,[8] leading also to a consideration of interactions between normal hydrophobic molecules and their perfluorinated analogues.[9] This paper provides an initial view of perfluoroalkane interactions with themselves and the *n*-paraffins as an extension of our recent study of binary alkane compositions.

Materials and Methods

Compounds. Two alkanes, 97% pure *n*-nonadecane, *n*-$C_{19}H_{40}$ (Aldrich Chemical Co., Milwaukee, WI), and 99.5% pure *n*-eicosane, *n*-$C_{20}H_{42}$ (Eastman Chemical Co., Rochester, NY), were used as standards for comparison with partially or fully perfluorinated alkanes of similar chain length. Their crystal structures are described by Nyburg and Potworowski.[10] All perfluoroalkanes, viz. perfluorododecane, *n*-$C_{12}F_{26}$, perfluorotetradecane, *n*-$C_{14}F_{30}$, perfluorohexadecane, *n*-$C_{16}F_{34}$, and perfluoroeicosane, *n*-$C_{20}F_{42}$, were purchased from PCR Inc. (Gainesville, FL) and are of unspecified purity. Diblock compounds such as 1-(perfluoro-*n*-dodecyl)-*n*-hexane, $CF_3(CF_2)_{11}(CH_2)_5CH_3$ (or $F_{12}H_6$), 1-(perfluoro-*n*-dodecyl)-*n*-octane, $CF_3(CF_2)_{11}(CH_2)_7CH_3$ (or $F_{12}H_8$), 1-(perfluoro-*n*-dodecyl)-*n*-decane, $CF_3(CF_2)_{11}(CH_2)_9CH_3$ (or $F_{12}H_{10}$), 1-(perfluoro-*n*-dodecyl)-*n*-dodecane, $CF_3(CF_2)_{11}(CH_2)_{11}CH_3$ (or $F_{12}H_{12}$), 1-(perfluoro-*n*-octyl)-*n*-dodecane, $CF_3(CF_2)_7(CH_2)_{11}CH_3$ (or F_8H_{12}), and 1-(perfluoro-*n*-decyl)-*n*-dodecane, $CF_3(CF_2)_9(CH_2)_{11}CH_3$ (or $F_{10}H_{12}$) were synthesized by Dr. Robert J. Twieg at IBM Almaden Research Center, San Jose, CA, and are at least 98% pure. Physical constants for these materials are listed in Table I.

Differential Scanning Calorimetry. Differential scanning calorimetry of 2-4 mg samples sealed in aluminum crucibles was carried out with a Mettler TA3300 instrument, generally at a heating or cooling rate of 5 °C/min. Binary samples were first fused just above the transition temperature of the highest melting component and then reheated after a slow cooling to room temperature. Transition enthalpies were calibrated against the value for indium and the temperature scale was adjusted to fit a polynomial curve through the melting temperatures for indium, lead, and zinc. Only peak values are used for plotting binary phase diagrams, including those for solid solutions.

Diffraction. Preliminary electron diffraction experiments were carried out on diblock compounds crystallized from hot toluene solution onto carbon-film-covered electron microscope grids. The electron microscope used was a JEOL JEM-100B7 operated at 100 kV and using normal low beam exposure conditions for radiation-sensitive compounds.

Low-angle X-ray diffraction measurements were made with a homemade slit-collimated camera for a Rigaku Rotaflex rotating anode X-ray generator with a Cu Kα source operated at 40 kV and 20 mA. Diffraction patterns were detected with a position-sensitive proportional counter. Samples used for diffraction experiments were taken from DSC pans after heating experiments were completed and the solid was packed in 1.0-mm diameter glass capillaries by centrifugation.

Calculations. For the binary combinations considered in this study the phase behavior was evaluated in terms of ideal solution theory. For two compounds that form eutectics in the solid state, this ideality is evaluated in terms of the depression of the freezing point T for an ideal solution according to the well-known Schröder equations:[11]

$$\ln X_{A,B} = -\frac{\Delta H_{A,B}}{R}\left(\frac{1}{T} - \frac{1}{T_{A,B}}\right) \quad (1)$$

where X_A and $X_B = 1 - X_A$ are the mole fractions of components A and B, R is the gas constant, $\Delta H_{A,B}$ is the transition enthalpy of pure A or B, and T_A and T_B are the melting points of the pure materials (on the Kelvin scale).

If the two compounds form a solid solution, then the melt-

0024-9297/90/2223-0894$02.50/0

Table I
Physical Data for Perfluoroalkanes and Perfluoroalkane/Alkane Diblock Molecules[c]

compd	T_1, °C (lit.)	ΔH_1, kJ/mol (lit.)	ls_1, Å (lit.)	T_2, °C (lit.)	ΔH_2, kJ/mol (lit.)	ls_2, Å (lit.)
$C_{12}F_{26}$				73.7 (71.3[a])	21.9 (23.0[a])	18.2[a] (17.9[b])
$C_{14}F_{30}$				103.7	31.4	20.4
$C_{16}F_{34}$				126.8	36.2	23.3 (23.1)
$C_{20}F_{42}$				162.1	47.6	28.6 (28.4)
$F_{12}H_6$	47.2 (44.0[a])	3.3 (3.3[a])		80.7 (79.0[a])	22.8 (21.8[a])	23.2 (24.8[a])
$F_{12}H_8$	50.4 (51.0)	6.3 (5.6)	39.0 (40.5[a])	83.3 (82.0)	18.9 (21.9)	26.7 (27.9)
$F_{12}H_{10}$	64.0 (66.0)	9.0 (7.5)	40.8 (42.9)	85.8 (84.0)	20.3 (22.2)	29.3 (30.7)
$F_{12}H_{12}$	79.0 (80.0)	11.2 (11.3)	43.0 (44.9)	90.3 (89.0)	25.9 (24.5)	25.4 (32.9)
F_8H_{12}				39.8	33.4	34.7
$F_{10}H_{12}$	64.0		40.3	85.6	36.2	33.8

[a] Reference 9 (note that earlier reported H should be in kJ/mol). [b] Reference 23. [c] ls = lamellar spacing.

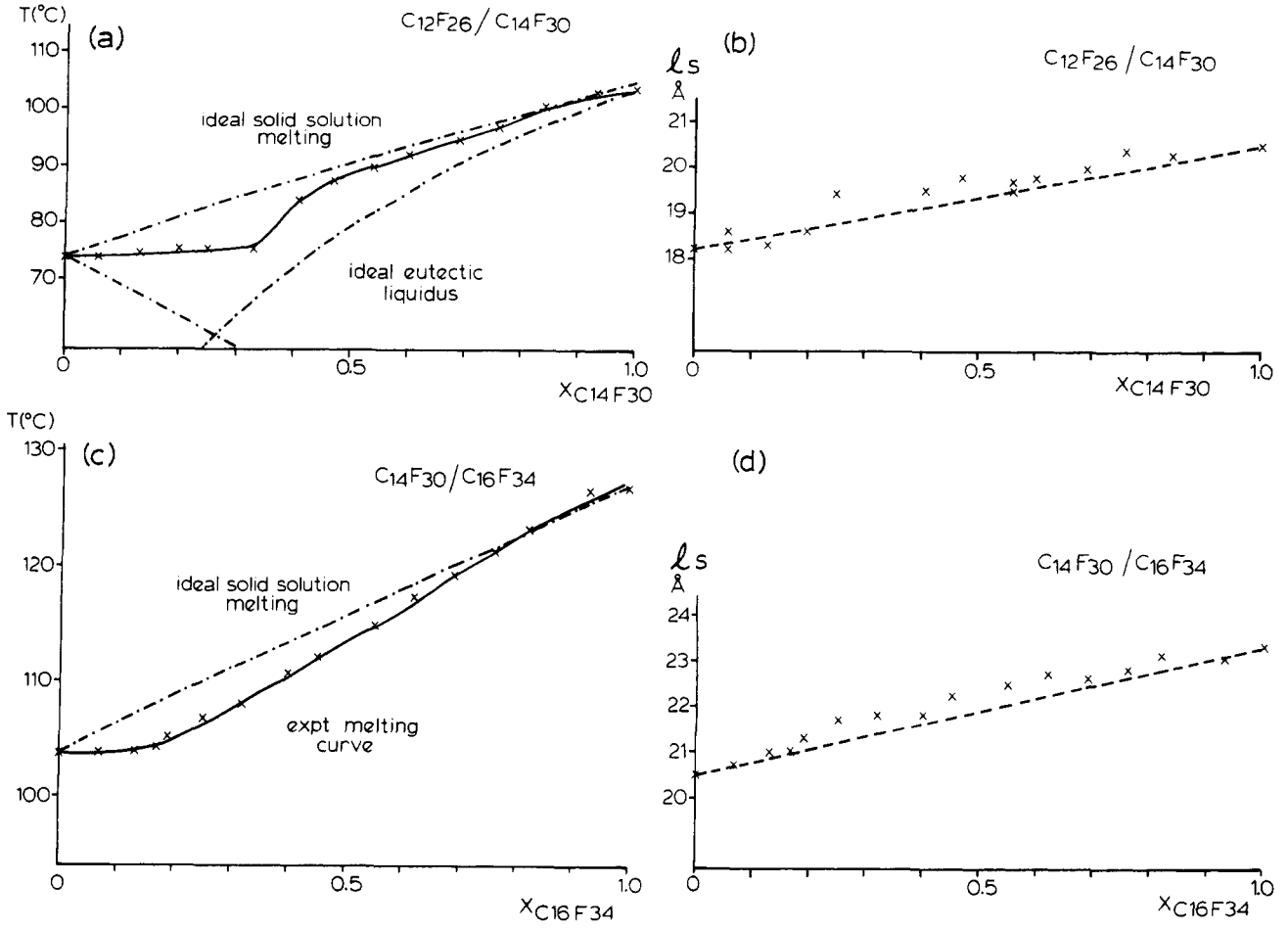

Figure 1. Thermal and diffraction data from perfluoroalkane solid solutions. $C_{12}F_{26}/C_{14}F_{30}$: (a) binary phase diagram (note that the experimental melting line (x) deviates from the ideal melting line calculated with eq 2 but is not near the eutectic liquidus curves calculated with eq 1; (b) the lamellar spacings mostly lie above the Vegard's law line connecting the lamellar spacings of the pure components. $C_{14}F_{30}/C_{16}F_{34}$: (c) the phase diagrams again indicate a deviation of the melting line from the ideal case as in (a); (d) the lamellar spacings are again continuous.

ing curve is dependent upon the mole fraction

$$\bar{X}_B = \frac{1}{2}(X_B^{(L)} + X_B^{(S)})$$

where

$$X_B^{(S)} = \frac{e^{-B} - 1}{e^{-A} - e^{-B}}$$

and

$$X_B^{(L)} = e^{-B} X_B^{(S)} \qquad (2)$$

based upon the definitions:[12]

$$e^{-A,B} = \exp\left[-\frac{\Delta H_{A,B}}{R}\left(\frac{1}{T} - \frac{1}{T_{A,B}}\right)\right]$$

Deviations from ideal behavior can be evaluated in terms of a lattice model such as the Flory–Huggins theory or alternatively models based on various formulations of the Bragg–Williams theory.[12-14] In the latter case, a term is employed to account for the nonzero heat of mixing with the empirical interaction term ρ_0 where $\Delta H_m = \rho_0 X_1 X_2$ such that

$$\frac{\rho_0(1 - X_1)^2}{\Delta H_1} = \frac{T}{T^{ideal}} - 1 \qquad (3)$$

For this correction the term T^{ideal} is the transition temperature obtained from the above relations based upon ideal theory.

Results

Binary phase behavior for n-paraffins has already been considered by us in five previous papers.[3,4,15-17] Nonideal eutectic behavior was considered in a paper on paraffin/

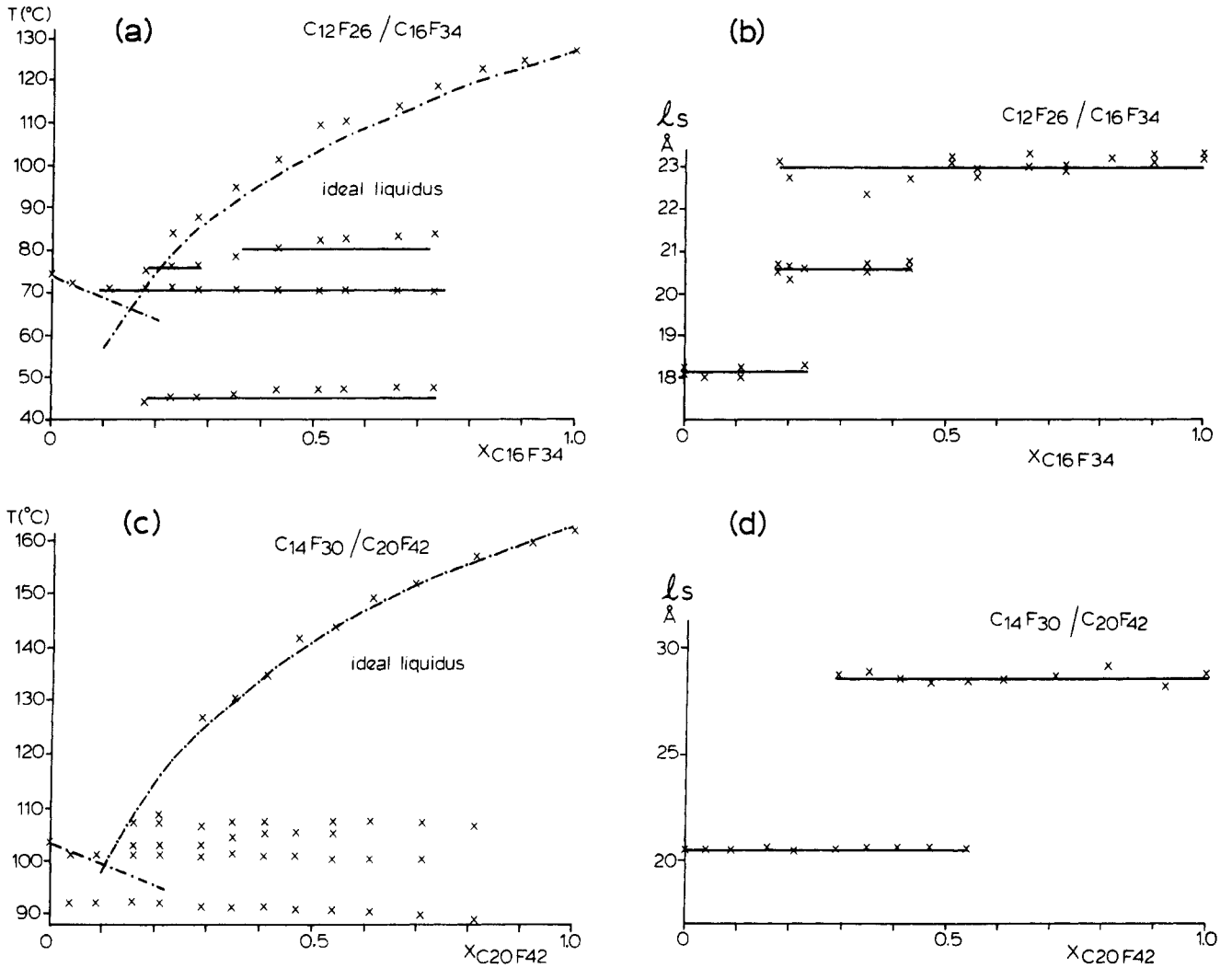

Figure 2. Eutectic interactions for perfluoroalkanes $C_{12}F_{26}/C_{16}F_{34}$: (a) phase diagram (the liquidus curve is well matched by using eq 1); (b) the lamellar spacings overlap for successive concentration domains. $C_{14}F_{30}/C_{20}F_{42}$: (c) phase diagram. (Again, the experimental liquidus curve is well matched by use of eq 1); (d) because there is no limited solubility, only two lamellar spacings, respectively from the pure components, are seen in the eutectic solid.

diluent solids.[18] In the following we consider pairwise interactions among compounds listed in Table I.

Perfluoroalkane/Perfluoroalkane. The reference crystal structure of perfluoroalkane is discussed by Bunn and Howells[19] for perfluorohexadecane, $C_{16}F_{34}$. The chain packing is in rectangular layers (i.e. axes normal to the lamellar surface), and the chain helical twisting is similar to that found for the infinite polymer.[19-21] The resultant average perfluoromethylene chain rotor in the projection down the chain axes has been the subject of a quantitative electron diffraction structure analysis, supporting earlier X-ray analyses.[22] A representative electron diffraction pattern has been published earlier.[22] The linear relationship between the chain length and lamellar spacing can be shown by plotting data in Table I. When a comparison can be made, our lamellar spacing values are very close to the ones found by Starkweather.[23] Combining our data with his, the spacing increment per difluoromethylene unit is 1.32 Å compared to the 1.33 Å value determined by him (1.0 Å ≡ 0.10 nm).

Two binary combinations, viz., $C_{12}F_{26}/C_{14}F_{30}$ and $C_{14}F_{30}/C_{16}F_{34}$, are found to form solid solutions as shown by the continuity of melting points in the binary phase diagrams and the continuity of lamellar spacings over a concentration series (Figure 1). Comparison to the ideal melting curves computed with eq 2 indicates, however, that the solid solutions are nonideal. It also appears from at least one stepwise increase of lamellar spacing with concentration for each series (Figure 1b,d) that prominent average crystal structures may dominate successive composition regions, an observation also made earlier for long chain alcohols.[24] Similar stepwise behavior is found on the microcrystalline level for *n*-alkanes.[3]

When the chain length difference changes from two to four perfluoromethylene units, the solid fractionates. The liquidus curve in the $C_{12}F_{26}/C_{16}F_{34}$ phase diagram is well fit by a calculation of ideal freezing point depression with eq 1 (Figure 2a). Note, however, that the isothermal solidus line does not extend all the way to the $X = 1.0$ concentration for the $C_{16}F_{34}$ component. The presence of three constant lamellar spacings from the low-angle X-ray data that overlap over the concentration range (Figure 2b) can be interpreted from earlier electron and X-ray diffraction measurements on binary paraffin solids[17] to mean that the secondary crystallization may consist of an incommensurate solid of randomly alternating lamellae of fractionated pure components. Thus the limited range of the solidus isotherm is consistent with the occurrence of a metastable solid solution at high concentrations of the $C_{16}F_{34}$ component, especially when crystallized from the melt, and this later fractionates.

Total separation of the components is achieved when

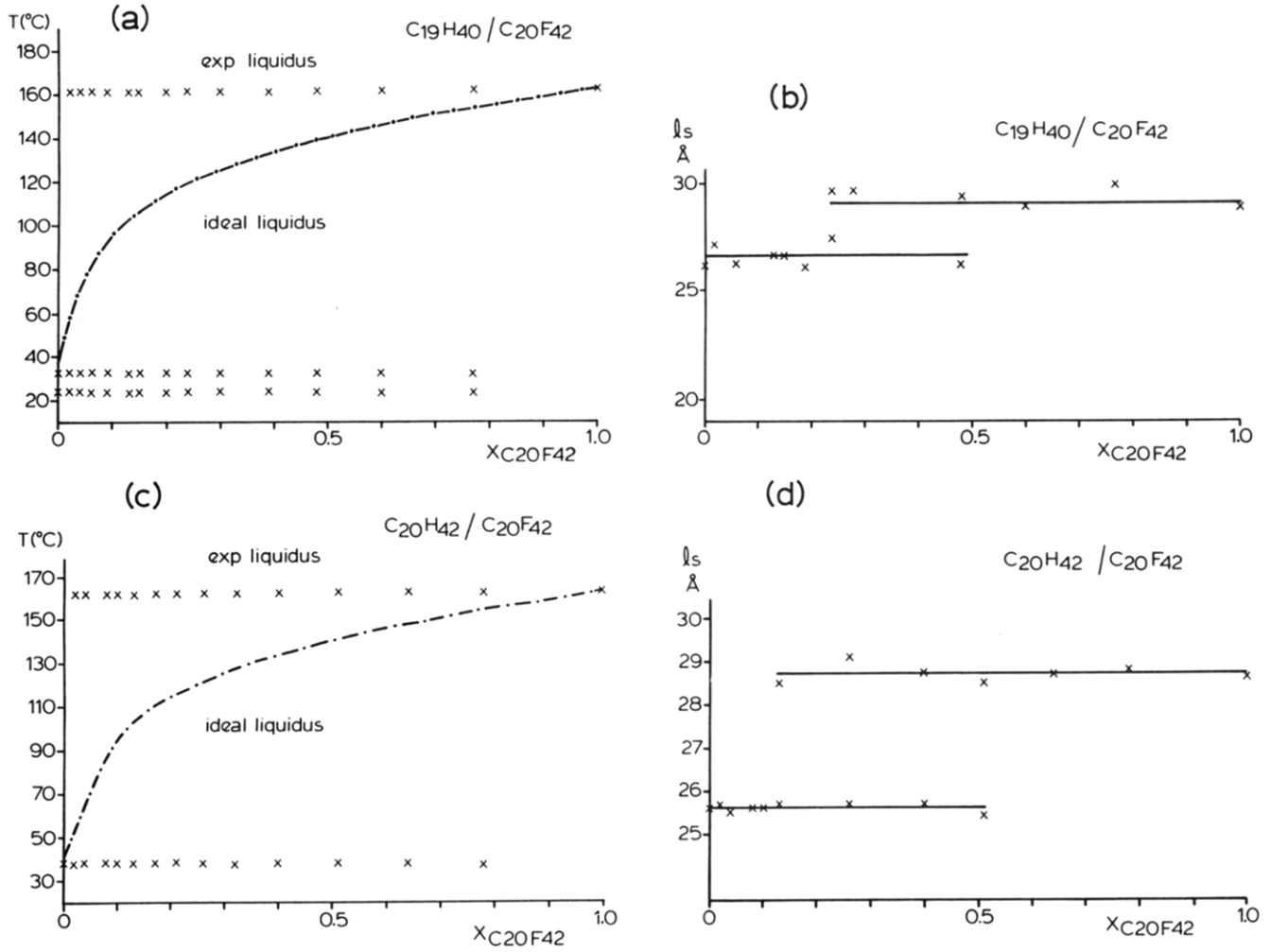

Figure 3. Thermal and X-ray diffraction data from alkane/perfluoroalkane binary solids. $C_{19}H_{42}/C_{20}F_{42}$: (a) phase diagram (the liquidus is an isotherm and does not correspond to the expected liquidus calculated from eq 1 assuming an ideal solution to be formed in the comelt); (b) lamellar spacings indicate total separation of the pure components. $C_{20}H_{42}/C_{20}F_{42}$; (c) phase diagram with behavior resembling (a); (d) lamellar spacings from the phase-separated components.

the chain length difference is six perfluoromethylene units, e.g. in $C_{14}F_{30}/C_{20}F_{42}$ solids (Figure 2c). Again, the liquidus curve is predicted by an ideal freezing point depression calculation. The X-ray diffraction patterns now contain only two overlapping spacings from the pure components (Figure 2d), consistent with the behavior for *n*-paraffins when the chain length difference is too great to allow formation of a metastable solid solution from the rapidly cooled comelt. In earlier work,[7] eutectic behavior also was found for $C_{12}F_{26}/C_{20}F_{42}$ combinations.

Perfluoroalkane/Alkane. If one were only to consider the great difference in melting points, then binary solids made up of perfluoroalkanes and alkanes of similar chain lengths are expected to be eutectics, as shown by the phase diagrams of $C_{19}H_{40}/C_{20}F_{42}$ and $C_{20}H_{42}/C_{20}F_{42}$ and also by the occurrence of two overlapping lamellar spacings from the pure components in low-angle X-ray diffraction patterns (Figure 3). However, the observed phase diagrams indicate yet another important property of these binary solids in that they are grossly nonideal in their melting behavior. The experimental liquidus curve is isothermal for both binary systems and completely unlike the curve calculated from the Schröder equation. Deviations from ideality in this direction have been found for paraffin/diluent solids[18] but not to the extreme seen here. The direction of the nonideality indicates that the individual pure components strongly prefer to associate only with themselves—even in the liquid state, which is

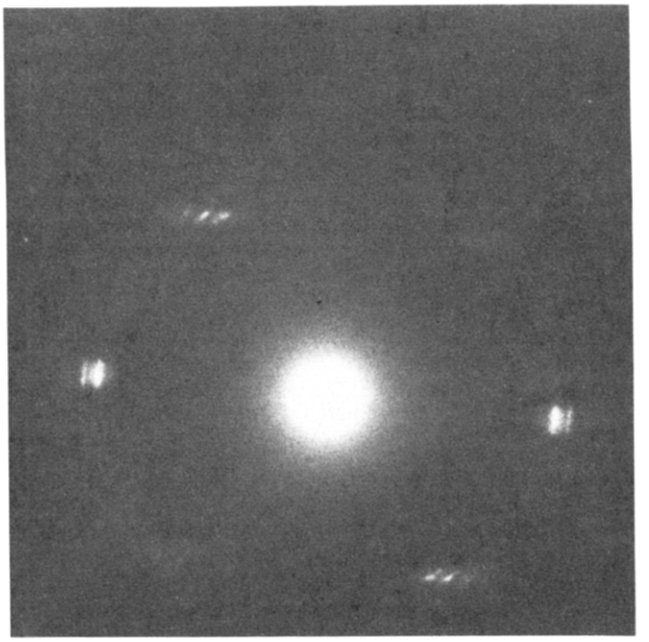

Figure 4. Electron diffraction pattern from $F_{12}H_{12}$ for which a tilted chain form is seen. Here the center of the most intense spots corresponds to the $d_1^* = (4.92 \pm 0.09\ \text{Å})^{-1}$ spacing of the perfluoroalkane chain structure. (Note that this is actually a superlattice with a spacing of 51.9 ± 1.0 Å.) The orthogonal dimension in the tilt direction is $d_2^* = (6.82 \pm 0.16\ \text{Å})^{-1}$.

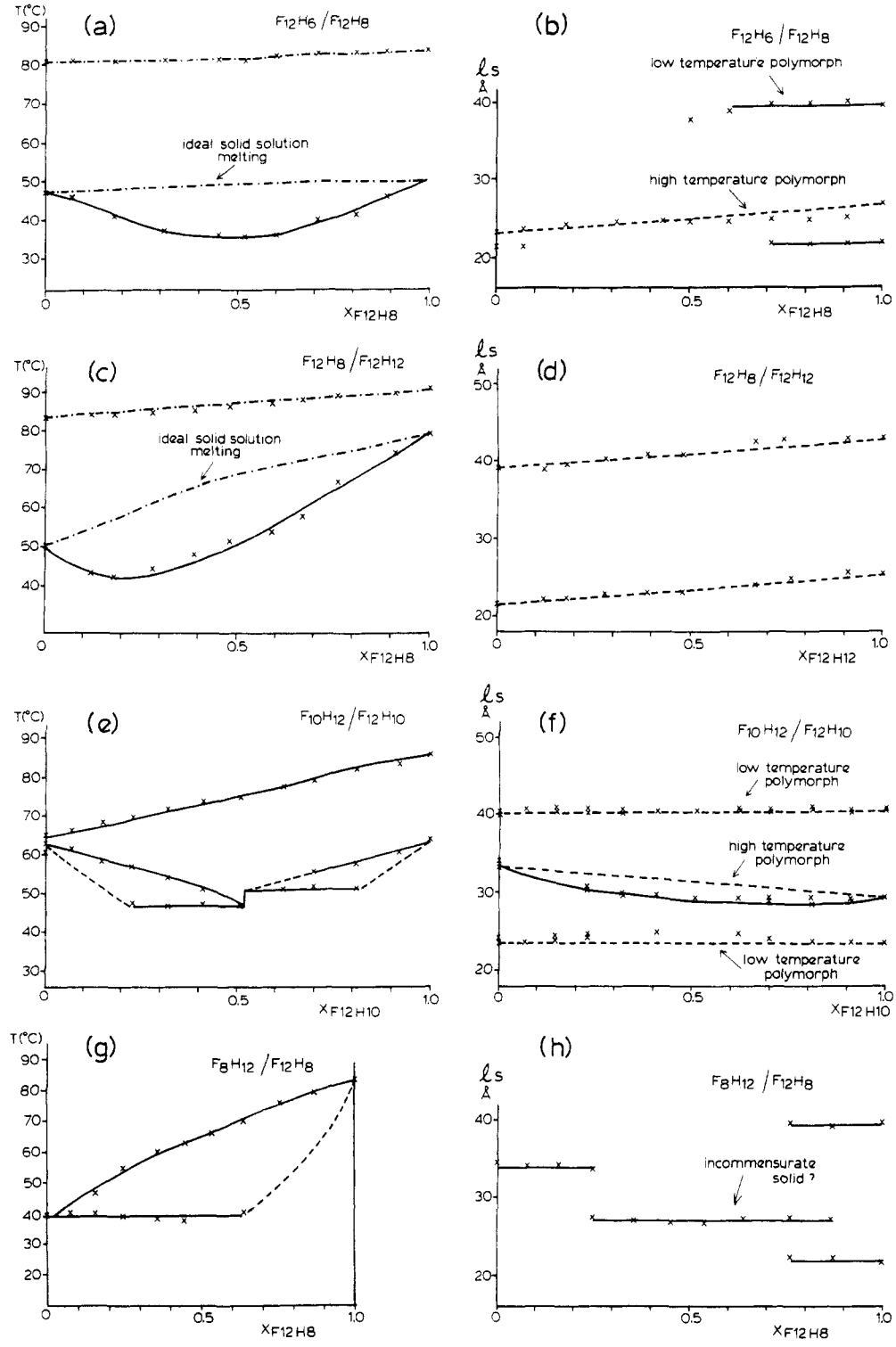

Figure 5. Thermal and diffraction data from diblock binaries. $F_{12}H_6/F_{12}H_8$: (a) binary phase diagram (the polymorphic transition at low temperature is nonideal whereas the melting curve corresponds very closely to the ideal curve calculated from eq 2); (b) lamellar data (the lower line due to the higher temperature polymorph is continuous with concentration; the low-temperature polymorph is only found with relatively large amounts of $F_{12}H_8$). $F_{12}H_8/F_{12}H_{12}$: (c) again, the phase diagram indicates the solid solution of the lower temperature is nonideal whereas that of the higher temperature form is nearly ideal; (d) lamellar spacings. $F_{12}H_{10}/F_{10}H_{12}$: (e) the binary phase diagram shows that a solid solution exists for the higher temperature polymorph whereas the lower temperature form fractionates; (f) lamellar spacings; $F_{12}H_8/F_8H_{12}$: (g) when the diblock combinations are more asymmetrical, the components fractionate, but with some solid solubility perhaps at higher concentrations of $F_{12}H_8$; (h) lamellar spacings.

found also to be a two-phase system upon observation in a light microscope with a heating stage.

Diblock/Diblock. The crystal structure of perfluoroalkane/alkane diblock compounds is still under investigation. For $F_{12}H_8$, one prominent electron diffraction pattern has been obtained which is identical to the one found for pure perfluoroalkanes.[22] The same pattern is also seen for $F_{12}H_8$. Hence the chains are untilted with a lateral hexagonal spacing, $d_{100}^* = (4.96\ \text{Å})^{-1}$. When the alkyl residue becomes longer, e.g. $F_{12}H_{12}$, the chains are often tilted (Figure 4). These results are not necessarily consistent with the low-angle X-ray diffraction data[9] (since two forms exist for $F_{12}H_8$, for example). Because the crystals are grown from hot solvent, a high-

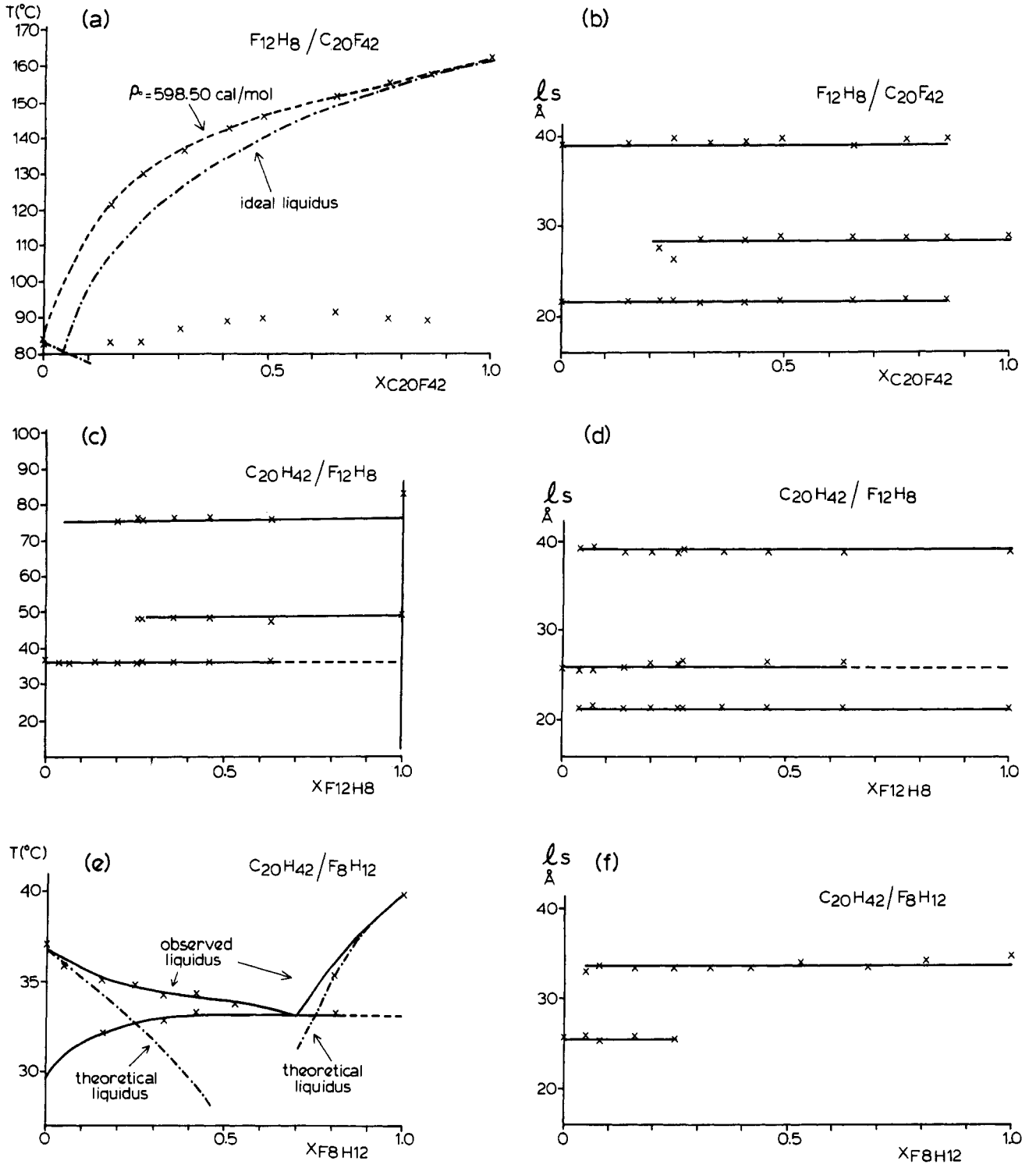

Figure 6. Diblocks combined with homogeneous chain compounds, $F_{12}H_8/C_{20}F_{42}$: (a) eutectic binary phase diagram (although the experimental liquidus line lies above the ideal line calculated from eq 1, an adjustment for nonideal behavior, assuming clustering of pure molecular species, fits the experimental curve); (b) lamellar spacings. $F_{12}H_8/C_{20}H_{42}$: (c) eutectic phase diagram with an isothermal liquidus line; (d) lamellar spacings. $F_8H_{12}/C_{20}H_{42}$: (e) eutectic phase diagram; (f) lamellar spacings.

energy form may be favored for some compounds. There also is a discrepancy between one lamellar spacing value and the value found in earlier studies (see $F_{12}H_{12}$ in Table I). It is known[9] that for the $F_{12}H_m$ series where $m \leq 6$, a single-crystal structure exists which is similar to one of the two coexistent chain packings when $8 \leq m \leq 12$ (favored at high temperature). If the fluorocarbon moiety is held constant at F_{12}, then binary combinations $F_{12}H_6/F_{12}H_8$ and $F_{12}H_8/F_{12}H_{12}$ form solid solutions. As shown by the phase diagrams in Figure 5a,c, the low-temperature forms exist as nonideal solutions while the solutions of the higher temperature polymorphs are more ideal (probably indicating the presence of molecular conformational disorder). Since the crystal structures are not known, it is difficult to interpret the low-angle spacings (Figure 5b,d).

Two other combinations were considered where the total chain length was conserved, but the order of block lengths was switched. In the binary solid $F_{12}H_{10}/F_{10}H_{12}$ the higher melting polymorphs form a solid solution but the lower melting crystal forms may fractionate (Figure 5e). For the even more asymmetric binary solid of $F_{12}H_8/F_8H_{12}$

a eutectic is clearly found with some initial cosolubility possibly occurring at high concentrations of $F_{12}H_8$ (Figure 5g). Again, an intermediate lamellar spacing may indicate the presence of an incommensurate solid of constant composition.

Diblocks with Homogenous Chain Compounds. Finally, it is interesting to see what happens when a diblock; e.g., $F_{12}H_8$ is associated with a linear compound which is either perprotonated or perfluorinated but retains the same chain length. The binary solid of $F_{12}H_8/C_{20}F_{42}$ is a eutectic (Figure 6a), as indicated also by X-ray diffraction data (Figure 6b). The experimental liquidus curve, however, although nonideal and indicating a preference for self-association of like molecules, is not so aberrant as the one depicted in Figure 3; i.e., the components would appear to be cosoluble in the liquid state. This is verified by observation in the light microscope. The relationship between $F_{12}H_8$ and $C_{20}H_{42}$ (Figure 6c), on the other hand, is more similar to the behavior of $C_{20}H_{42}/C_{20}F_{42}$ since the liquidus curve again is virtually horizontal. Fractionation of the comelt is, in fact, observed. The binary solid between F_8H_{12} and $C_{20}H_{42}$, although nonideal (Figure 6e), indicates that the compounds are cosoluble in the melt as verified by light microscopy. Perhaps some cosolubility exists for high concentrations of the alkane in the solid state.

Discussion

For binary combinations of the pure perfluoroalkanes, conditions for cosolubility in the solid state is shown to encompass small differences in molecular volume. In fact, the chain length difference that can form a stable solid solution is very similar to the case of the *n*-paraffins. Using the empirical formula found by Matheson and Smith,[25] i.e.

$$C_N^{\max} = 1.224C_N^{\min} - 0.411$$

to define the boundary of the stable solid solutions, one can, in fact, also predict the observed chain length differences that are possible in cosoluble perfluoroalkane solids. Nevertheless, unlike the case of the *n*-alkane binaries, the melting lines for the perfluoroalkane solutions deviate from ideal behavior. It is interesting to note that when the permissible molecular volume difference is exceeded so that cosolubility can be found only at high concentrations of the longer chain component, e.g. in $C_{12}F_{26}/C_{16}F_{34}$, the secondary solid, probably a superlattice-like incommensurate solid with invariant composition, is formed when the solidus line is crossed, as indicated by the intermediate lamellar spacing. Such behavior has been characterized in detail for *n*-paraffins.[4] Again, like paraffin binaries, the separate crystallization of the two components occurs only when they are completely insoluble, e.g. in $C_{14}F_{30}/C_{20}F_{42}$ solids and, undoubtedly, for the $C_{12}F_{26}/C_{20}F_{42}$ solids considered earlier.[7] In our model calculations we find that the liquidus curve is well fit by assuming that ideal liquid solutions are being cooled to their freezing point, a result again similar to the behavior found earlier for $C_{12}F_{26}/C_{20}F_{42}$ binaries.[7]

As is well-known, fluorocarbons and hydrocarbons are mutually insoluble. This is demonstrated by the rather bizarre isothermal liquidus curves for n-$C_{19}H_{40}/nC_{20}F_{42}$ and n-$C_{20}H_{42}/nC_{20}F_{42}$ which are actually the isothermal phase transition lines for phase-separated liquids. As stated above, the phase separation in the liquid phase can be visualized with a heating stage on a light microscope. The combination of alkane and fluoroalkane segments on a single chain thus comprises a detergent. For example, amphiphile-like properties were found[26] when diblocks of the type $F_{12}H_m$, where m = 8–20, were combined with decane in that gels were formed. Such an interaction was also found in combinations of $F_{10}H_{12}$ with various hydrocarbon solvents that were either rings or linear molecules. Although we have not specifically observed the formation of gels, the occurrence of an isotropic liquid phase for $F_8H_{12}/C_{20}H_{42}$ and $F_{12}H_8/C_{20}F_{42}$ binaries indicate that the detergent behavior is favored when a dominant functional group of the diblock would be soluble in the second component. When the functional group is too small, e.g. in $F_{12}H_8/C_{20}H_{42}$ binaries, an isotropic liquid phase cannot form. Combinations of these diblocks in binary solids should allow cosolubility to occur within allowable chain length differences for the sequestered molecular domains; i.e. $F_{12}H_6/F_{12}H_8$ and $F_{12}H_8/F_{12}H_{12}$ binaries allow the formation of solid solutions, although they are grossly nonideal for the low-temperature polymorph. Similar rules are in force for the asymmetric diblocks. For example, the binary $F_{10}H_{12}/F_{12}H_{10}$ is partially fractionated for the low-temperature form, whereas the more asymmetric $F_{12}H_8/F_8H_{12}$ is a eutectic.

When a diblock is found to be cosoluble with either an alkane or a perfluoroalkane in the melt, the liquidus curve in the phase diagram is nevertheless nonideal in contrast to the case when two like species with dissimilar molecular volumes form an eutectic (e.g. Figure 2a,c). The deviation of the observed liquidus from the one calculated with the Schröder equation (1) for the binary series $F_{12}H_8/C_{20}F_{42}$ is shown in Figure 6a. Correction of the ideal theory for nonzero mixing enthalpy using the Bragg–Williams theory (eq 3) leads to an interaction constant of ρ = 598.5 cal/mol to produce a close match to the experimental curve. The positive sign of this term indicates that the pure species tend to cluster in the liquid phase,[14] consistent with the observations made above.

Although perfluorinated alkanes are not wet by either typical hydrophobic molecules or polar ones, the binary phase interactions are similar to the hydrogenated *n*-paraffins. A concept of detergency can be defined, therefore, for the diblocks comprised of alkane/perfluoroalkane segments for which "fluorophile" segments will replace the usual hydrophilic moiety of such an amphiphilic molecule.

Acknowledgment. Research was supported by a grant from the National Science Foundation (DMR86-10783). The author is grateful to Dr. Robert J. Twieg for his gift of the diblock compounds used in this work. He also thanks Dr. Twieg and Dr. John F. Rabolt of the IBM Almaden Research Laboratory for useful discussions of the results.

References and Notes

(1) Mnyukh, Yu. V. *Zh. Strukt. Khim.* **1960**, *1*, 370.
(2) Kitaigorodskii, A. I. *Organic Chemical Crystallography*; Consultants Bureau: New York, 1961; p 231 ff.
(3) Dorset, D. L. *Macromolecules* **1987**, *20*, 2782.
(4) Dorset, D. L. *Macromolecules* **1986**, *19*, 2965.
(5) Maroncelli, M.; Strauss, H. L.; Snyder, R. G. *J. Phys. Chem.* **1985**, *89*, 5260.
(6) Kim, Y.; Strauss, H. L.; Snyder, R. G. *J. Phys. Chem.* **1989**, *93*, 485.
(7) Smith, P.; Gardner, L. H. *Macromolecules* **1985**, *18*, 1222.
(8) Rabolt, J. F.; Russell, T. P.; Twieg, R. J. *Macromolecules* **1984**, *17*, 2786.
(9) Russell, T. P.; Rabolt, J. F.; Twieg, R. J.; Siemens, R. L.; Farmer, B. L. *Macromolecules* **1986**, *19*, 1135.
(10) Nyburg, S. C.; Potworowski, J. A. *Acta Crystallogr.* **1973**, *B29*, 347.
(11) Hsu, E. C.-H.; Johnson, J. F. *Mol. Cryst. Liq. Cryst.* **1974**, *27*, 95.

(12) Lee, A. G. *Biochim. Biophys. Acta* **1977**, *472*, 285.
(13) Tenchov, B. G. *Prog. Surf. Sci.* **1985**, *20*, 273.
(14) Gordon, P. *Principles of Phase Diagrams in Materials Systems*; McGraw-Hill: New York, 1968; p 79 ff.
(15) Dorset, D. L. *Macromolecules* **1985**, *18*, 2158.
(16) Dorset, D. L. *J. Polym. Sci., Polym. Phys. Ed.* **1989**, *27*, 1161.
(17) Dorset, D. L. *Macromolecules*, in press.
(18) Dorset, D. L.; Hanlon, J.; Karet, G. *Macromolecules* **1989**, *22*, 2169.
(19) Bunn, C. W.; Howells, E. R. *Nature* **1954**, *174*, 549.
(20) Clark, E. S.; Muus, L. T. *Z. Kristallogr.* **1962**, *117*, 108.
(21) Clark, E. S.; Muus, L. T. *Z. Kristallogr.* **1962**, *117*, 119.
(22) Dorset, D. L. *Chem. Phys. Lipids* **1977**, *20*, 13.
(23) Starkweather, H. W., Jr. *Macromolecules* **1986**, *19*, 1131.
(24) Amelinckx, S. In *Growth and Perfection of Crystals*; Doremus, R. H., Roberts, B. W., Turnbull, D., Eds.; Wiley: New York, 1958; p 586.
(25) Matheson, R. R., Jr.; Smith, P. *Polymer* **1985**, *26*, 288.
(26) Twieg, R. J.; Russell, T. P.; Siemens, R.; Rabolt, J. F. *Macromolecules* **1985**, *18*, 1361.

Notes

Dynamic Behavior in Ternary Polymer Solutions. Concentration Dependence of Diffusion Coefficients

W. BROWN,* C. KOŇÁK, R. M. JOHNSEN, AND P. ZHOU

Institute of Physical Chemistry, University of Uppsala, Box 532, 751 21 Uppsala, Sweden. *Received May 16, 1989; Revised Manuscript Received July 18, 1989*

Benmouna et al.[1] have developed a theory for dynamic light scattering from ternary mixtures of two homopolymers and a solvent, based on previous results for the elastic scattering from such systems. Using the random-phase approximation, their approach is to write down in matrix form the dynamic structure factor in terms of the intensity contributions from the individual species and the direct interactions between them. It is assumed that the Zimm type of hydrodynamic interactions are screened in the semidilute region and the hydrodynamic interactions between different molecules are not taken into account. Two examples were given: (A) two interacting polymers of the same size but having different contrast factors; (B) two monodisperse polymers differing in molecular weight but otherwise identical.

They were able to show that, in each case, two relaxation modes are obtained, and these were interpreted as the cooperative and interdiffusion modes, respectively (given in terms of the relaxation rates Γ_C and Γ_I). In contrast to the earlier reports of Phillies[5] and Pusey et al.,[6] Benmouna et al.[1a] give explicit expressions for the relaxation rates Γ_I and Γ_C as a function of the excluded-volume term: $2A_2M_wC$, where A_2 is the second virial coefficient and M the molecular weight. It should be noted that the theory as given is limited to interacting chains for which the second virial coefficient is nonzero, and therefore no provision was made for transport in Θ systems. Borsali[1d] has recently extended the discussion to include Θ systems.

It is of some relevance to compare the theoretical predictions for the relaxation rates with the results of experiments. We have recently[2] performed experiments dealing with case B, but employing only trace amounts of the one species (the "probe" chain) so that the interdiffusion coefficient approximately equals the self-diffusion coefficient of the probe. This point was confirmed in ref 2 where it is shown that, over the range of matrix concentration used, there is close agreement between the probe diffusion coefficients and the self-diffusion coefficients measured using pulsed-field-gradient NMR.

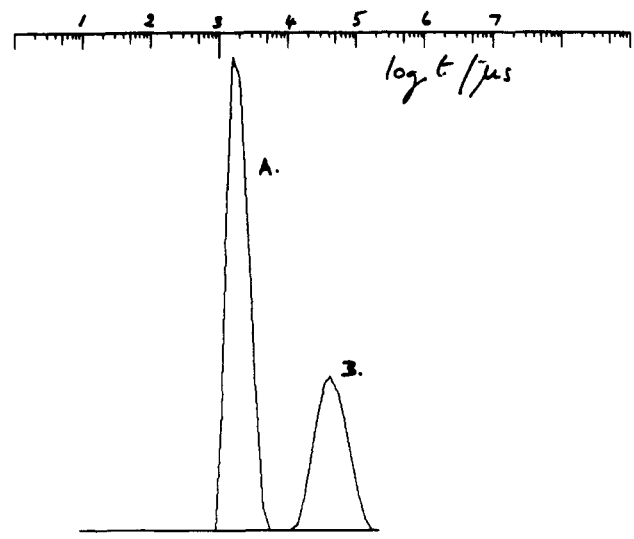

Figure 1. Decay time distributions for the ternary PIB system: for the PIB probe chain (B) ($M = 2.5 \times 10^5$) in a matrix (A) of PIB ($M = 4.9 \times 10^6$). Measurement angle 20°. Concentration of matrix 2×10^{-3} g·mL^{-1}.

Measurements were made on the two extremes: large probe chain in low molecular weight matrix and vice versa. In the present note, which complements the detailed paper,[2] we describe results on the previously examined polyisobutylene (PIB) system: A (PIB 4.9×10^6)/B (PIB 2.5×10^5)/chloroform. These two fractions have polydispersity indices $M_w/M_n \approx 1.2$. The following were used: (1) trace amount (≈0.05%) of A in semidilute solutions of B; (2) trace amount of B in semidilute solutions of A.

These experiments became feasible due to two recent innovations:

(a) the development of a broad-band autocorrelator (ALV multibit, multi-τ instrument allowing 23 simultaneous sampling times and having 191 exponentially spaced channels);

(b) implementation of a new program (REPES(3)) for performing Laplace inversion to obtain the decay time dis-

0024-9297/90/2223-0901$02.50/0